Acta Biochim Biophys Sin 2012, 44: 597–605 | © The Author 2012. Published by ABBS Editorial Office in association with Oxford University Press on behalf of the Institute of Biochemistry and Cell Biology, Shanghai Institutes for Biological Sciences, Chinese Academy of Sciences. DOI: 10.1093/abbs/gms041.
Advance Access Publication 1 June 2012

Original Article

# A faster immunofluorescence assay for tracking infection progress of human cytomegalovirus

Yingliang Duan[1], Lingfeng Miao[1], Hanqing Ye[1], Cuiqing Yang[1], Bishi Fu[1], Philip H. Schwartz[2], Simon Rayner[1], Elizabeth A. Fortunato[3]*, and Min-Hua Luo[1]*

[1]State Key Laboratory of Virology, Wuhan Institute of Virology, Chinese Academy of Sciences, Wuhan 430071, China
[2]National Human Neural Stem Cell Resource, Children's Hospital of Orange County Research Institute, Orange, CA 92868, USA
[3]Department of Biological Sciences and the Center for Reproductive Biology, University of Idaho, Moscow, ID 83844-3052, USA
*Correspondence address. Tel/Fax: +86-27-87197600; E-mail: Luomh@wh.iov.cn (M.L.)/Tel: +1-208-885-6966; Fax: +1-208-885-6518; E-mail: lfort@uidaho.edu (E.F.)

**Immunofluorescence assay (IFA) is one of the most frequently used methods in the biological sciences and clinic diagnosis, but it is expensive and time-consuming. To overcome these limitations, we developed a faster and more cost-effective IFA (f-IFA) by modifying the standard IFA, and applied this method to track the progression of human cytomegalovirus (HCMV) infection in different cells. The f-IFA that we developed not only saves time, but also dramatically reduces the quantity of antibody (Ab), which will facilitate the application of IFA in clinic diagnosis. f-IFA requires only 15 min for blocking, 10 min incubation for each primary and secondary Abs, followed by 1 min extensive wash after each incubation. Only 25 μl of diluted Ab solution was needed for each coverslip at the primary and secondary Ab incubation steps. In addition, all steps were performed at room temperature. This f-IFA has been applied successfully to follow virion entry (pp65) and expression of viral genes (IE1, UL44, and pp65) in order to track the details of HCMV infection process. We found that ∼0.5% HCMV-infected T98G cells formed multiple-micronuclei (IE1 and nucleus staining) and had virus shedding (pp65 staining) by f-IFA, which could not be detected by the traditional IFA. Our results indicated that f-IFA is a sensitive, convenient, fast, and cost-effective method for investigating the details of virus infection progress, especially HCMV infection. The faster and cost-effective feature with higher sensitivity and specificity implies that f-IFA has potential applications in clinical diagnosis.**

*Keywords* immunofluorescence assay; human cytomegalovirus; virus entry; viral gene expression; virus replication

Received: February 7, 2012 Accepted: April 5, 2012

## Introduction

Immunofluorescence assay (IFA) is frequently used in cellular and molecular biology to demonstrate the locations and functions of target proteins (e.g. cellular and non-cellular, intracellular and membrane, endogenous and exogenous proteins) [1,2]. There are two approaches for preparing samples used in IFA. The first method uses cells [2] or microbes [1] that are dropped, dried, and fixed on coverslips/slides; the second method uses adherent cells that are grown directly on coverslips [3,4], maintaining the natural cell morphology and showing the position of the target protein more clearly and accurately. Additionally, the IFA methods can be classified into direct immunofluorescent assay (dIFA) and indirect immunofluorescent assay (iIFA) according to the antibodies (Abs) used for detection. In dIFA, the fluorescence dye is conjugated to a primary Ab which specifically binds to the target protein. A fluorescent signal is detected when the dye is activated by the light of appropriate wavelength. In iIFA, a secondary Ab, which specifically binds to the primary Ab, is conjugated with a fluorophore which is similarly activated by excitation radiation.

The staining of IFA includes blocking, Ab incubation, and their intervening washes. The limiting factors of the staining stage are the length of time and the volume/quantity of the Ab. The major shortcomings of current IFAs are that they are time-consuming and expensive; the time for each incubation and wash can extend to several hours, and the volume of Ab solution can be as much as milliliters [4,5]. Thus, although useful, IFA is not cost effective in clinical diagnosis and it is necessary to improve the efficiency of IFA.

Our goals were to overcome these limitations, by developing a faster, more convenient, and cost-effective IFA

method, and apply the improved method to tracking human cytomegalovirus (HCMV) infection, namely following viral gene expression and determining location of viral antigens (proteins). In turn, it should be possible to track the infection process in HCMV-infected cells and has the potential for pathological diagnosis in clinics. The f-IFA method that we have developed was modified from the standard iIFA method for cells grown and fixed on coverslips [4,5], which has been proved to be sensitive and specific for virus infection detection but has the drawback of being time-consuming and expensive. In our method, cells were cultured and mock- or virus-infected as previously described [6–8], and the coverslips were harvested at the indicated time points followed by fixation and permeabilization [7]. The significant differences in our f-IFA protocol include the following: (i) During the whole f-IFA process, the coverslips were laid face down onto the incubation solution toward the parafilm membrane, which greatly increased the efficiency of fetal bovine serum (FBS) blocking and Ab reactions, so that the staining time and amount of Abs were dramatically reduced. (ii) We adopted an extensive and quick wash with force and quickly repeated dunking in the washing buffer, which greatly increased the wash efficiency. (iii) All these operations and reactions were carried out at room temperature (RT), except for storing samples and reagents at 4°C and temporarily keeping reagents on ice. (iv) No additional equipment is required, such as a 37°C incubator and a shaker. Our results demonstrated that the f-IFA protocol is significantly faster and uses less Abs compared with any other IFA methods [2–5].

## Materials and Methods

### Antibodies

Anti-UL44 monoclonal antibody (mAb) (IgG1) (1 : 1000) and anti-pp65 mAb (IgG1) (1 : 1500) were purchased from Rumbaugh-Goodwin Institute for Cancer Research, Inc. (Sykesville, USA). Anti-IE1 mAb (IgG2a) (1 : 1000) was a kind gift from Bill Britt, the University of Alabama (Birmingham, USA). Anti-GFAP mAb (IgG2b) (1 : 1000) was from NeoMarkers Inc. (Waltham, USA). The secondary Abs TRITC-conjugated goat-anti-mouse IgG1 and IgG2a Abs (1 : 250) were from Jackson ImmunoResearch Laboratories (West Grove, USA). Alexa 488-conjugated goat-anti-mouse IgG1, IgG2a, and IgG2b Abs (1 : 5000) were from Molecular Probes (Eugene, USA). The nuclear dye Hoechst 33258 (1 : 5000) was purchased from Sigma-Aldrich (St Louis, USA). All Abs and Hoechst 33258 were freshly diluted just before use in basic blocking solution [BBS, 1% BSA and 0.01% Tween-20 in phosphate-buffered saline (PBS)].

### Cells and cell culture

Cells with different permissiveness for HCMV infection were used. Human embryonic lung fibroblasts (HEL) and neural progenitor cells (NPCs) are primary cells and are fully permissive for HCMV infection; and T98G is a glioblastoma cell line that is semi-permissive for HCMV infection. These cells were cultured on coverslips as described previously [7–10]. Briefly, the poly-D-lysine uncoated (for HEL) or -coated (for T98G and NPCs) were placed in the dishes, and the cells were then plated onto the dishes. HEL and T98G cells were cultured in minimal essential medium (Gibco/BRL, Gaithersburg, USA) supplemented with 10% FBS, penicillin (100 U/ml) and streptomycin (100 μg/ml), L-glutamine (2 mM). NPCs were cultured in half changed growth medium (GM). GM is Dulbecco's modified Eagle's medium-F12 containing L-glutamine (2 mM Glutamax; Gibco/BRL), the antibiotics penicillin/streptomycin (100 U/ml and 100 μg/ml), gentamicin (50 μg/ml), amphotericin B (Fungizone; Gibco/BRL; 1.5 μg/ml), 10% BIT9500 (Stem Cell Technologies, Vancouver, Canada), human basic fibroblast growth factor (Invitrogen, Carlsbad, USA; 20 ng/ml), and human epithelial growth factor (Invitrogen; 20 ng/ml). Cells were maintained at 37°C in a 100% humidified atmosphere containing 5% $CO_2$.

### Viruses and virus infection

Virus strains of HCMV, Towne (ATCC VR-977) and AD169 (ATCC VR-538), were used for infection. NPCs and T98G cells were infected with Towne strain at a multiplicity of infection (MOI) of 3 and 10, respectively, and HEL cells were infected with AD169 strain at an MOI of 5. The cells grown on coverslips were mock- or virus-infected and harvested at the indicated time post infection (pi).

### Faster IFA

*Preparation of coverslip samples*. Coverslips were collected from the culture dishes with sharp, flame-sterilized forceps, and placed in 12-well plates filled with PBS. After being washed, the samples were fixed with 1 ml of fixation buffer [3% (vol/vol) formaldehyde in PBS] for 10 min at RT. Subsequently, the fixation buffer was aspirated and coverslips were rinsed twice with PBS. The fixed coverslips can be stored at 4°C in PBS. For permeabilization, the PBS in the wells was removed and 1 ml permeabilization buffer (1% Triton X-100 in PBS) was added into each well, statically incubated for 5 min, then the permeabilization buffer was aspirated and the coverslips were extensively rinsed with PBS.

*Immunofluorescent staining*. Before staining, a piece of parafilm membrane of the desired length was placed on the bench. To prevent the parafilm from moving during the

staining process, the parafilm was tightly attached onto the bench via a thin film of water formed by a few drops of water. The area for each coverslip was marked with a marker pen/sharpie and three plastic beakers were filled with PBS (100 ml) [**Fig. 1(A)**]. The immunofluorescent staining consisted of blocking, and sequential incubation with primary and secondary Ab solutions; each step was followed by a quick and extensive wash [**Fig. 1(B)**]. (i) *Blocking*: 30 μl blocking solution (BS, 30% FBS in BBS) was added in each defined area, the washed coverslip was placed (face down) above the pre-laid BS, allowing one edge to touch the BS and then the coverslip was slowly released to avoid the introduction of air bubbles [**Fig. 1(B)**]; the coverslip was then blocked for 15 min. Sufficient PBS was then added at the edge of the coverslip to dilute the BS and float the coverslip [**Fig. 1(C)**]. One coverslip was picked up and washed sequentially in the three beakers of PBS by repeatedly dunking. The excess PBS was drained on a paper tissue. (ii) *Incubation with primary Abs*: 25 μl of primary Ab solution was placed in the respective area and the washed coverslip was placed onto the solution as in the blocking step. Coverslips were incubated for 10 min, then the reaction was stopped with PBS and the coverslip was washed as in the blocking step. (iii) *Incubation with secondary Abs*: 25 μl of secondary Abs solution containing nuclear counterstaining dye Hoechst 33258 was placed in the respective area. Washed coverslip was placed onto the solution. The incubation, reaction stop, and wash were identical to the incubation with primary Abs.

*Mounting coverslips*. The slides were cleaned and marked, and anti-fade mounting solution (1‰ *p*-phenylenediamine in 90% glycerol) was added onto the slide; then the washed and drained coverslips were loaded (face down) on top of the anti-fade mounting solution, and gently pressed with forceps to squeeze out the extra solution. The excess anti-fade mounting solution was aspirated away by gentle vacuuming. The coverslips were sealed with nail polish and observed under a fluorescence microscope (Nikon, Tokyo, Japan).

### Application of f-IFA to track the progression of HCMV infection in different cells

The mock- or virus-infected cells on coverslips were harvested at the indicated time pi, and processed throughout fixation, permeabilization, and immunostaining. f-IFA was applied to track HCMV fully permissive infection progress in HEL, infection in T98G, and cytoskeleton change/cytopathic effects (CPE) in NPCs.

## Results

### Selection of incubation and washing conditions

There are two options that are currently used for the incubation step with Abs: the coverslips facing up or facing down. We selected the facing down option because it required less volume of Ab solution and potentially provided a more even distribution across the coverslip surface. For the post-incubation washing, there are also multiple ways to carry out. The most common method is to place each coverslip in an individual well in a 12-well plate and flood the well with PBS, rotate for 10 min, repeating 3 times. This method requires longer time and abundant wash buffer. The quick and extensive wash by sequentially dunking the coverslips in three beakers of PBS required only 1 min [**Fig. 1(A,B)**]. The results have shown that equally high-quality images could be achieved by both methods of washing (data not shown).

### Optimization of solution volume and incubation time

To optimize the solution volume, volumes from 15 to 50 μl with increments of 5 μl were tested. A volume of 15 μl was not sufficient to cover the whole coverslip; 20 μl was enough for incubation, but it was not easy to add PBS to stop the incubation and float the coverslip;

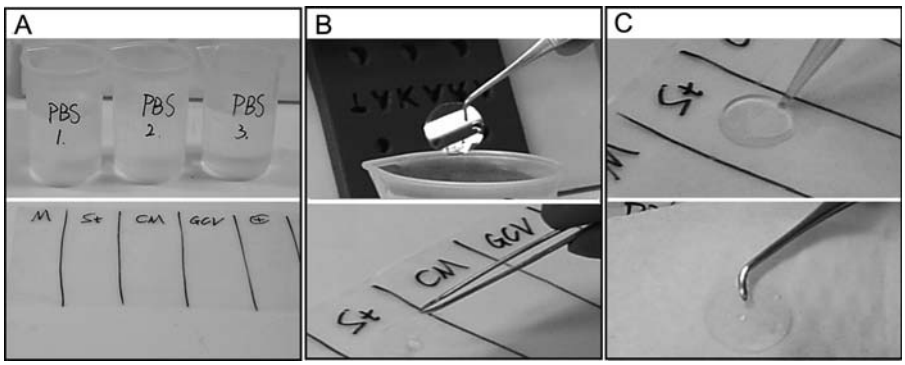


**Figure 1 Demonstration of experimental operations** (A) Set up the beakers and parafilm membrane. (B) Quick and extensive wash (up) and lay a coverslip facing down on the solutions (BS, primary and secondary Abs) for incubation (down). (C) Stop reaction and float the coverslip by adding PBS at the edge of the coverslip with a 1000 μl tip (up), and absorb redundant buffer by Kimwipe paper (down).

increasing the volume to 25 μl overcame these shortages [**Fig. 1(C)**]; 30 μl and higher volumes did not increase the strength of signal or further reduce the background. Finally, 25 μl was selected as the minimum effective volume.

To optimize the incubation time (i.e. the blocking and Ab incubation time), time periods of 5, 10, 15, 20, 25, 30, 40, 50, and 60 min were investigated. For the blocking step, 5 or 10 min was not enough to block the non-specific reactivity; 15 min incubation could enhance the blocking efficiency compared with 10 min, and completely blocked the non-specific reactivity; 20 min and longer time blocking had similar blocking efficiency as 15 min. Thus, 15 min was selected as the minimum effective blocking time. The incubation time periods for primary and secondary Ab were similarly determined. Incubating 5 min for both primary and secondary Ab did not produce sufficient specific signal, 10 min incubation increased the strength of the specific signal; 15 min and longer time incubations produced similar results compared with 10 min incubation. Thus, 10 min incubation was selected as the minimum effective time.

To evaluate the image quality from different IFAs, we observed HEL infected with Towne strain at 48 h pi. We used the same Ab dilutions. All the images were taken under the same conditions after staining without any adjustment. The exposure time was 30 ms for Hoechst, 30 ms for IE1, 40 ms for UL44, and 80 ms for phase images. The representative images obtained by f-IFA (Abs incubating for 5, 10 min) and traditional IFA are presented in **Fig. 2**. The mock-infected images are shown in **Fig. 2(A)**. It was obvious that f-IFA with 10 min Abs incubation had strong enough specific signal and showed distinct staining for IE1 and UL44 foci [**Fig. 2(B)**]; while the specific signal was not strong enough when incubating for only 5 min [**Fig. 2(C)**]; but incubating for 15 min just enhance the specific signal a little than incubating for 10 min (data not shown). The specific signal by traditional IFA was a little stronger than by f-IFA with 10 min Abs incubation, but it took 1 h for incubation [**Fig. 2(D)**], and this kind of weak signal could be easily overcome by exposing for longer time. Based on these results, we determined that the 10 min incubation time for f-IFA was suitable.

### Tracking the virus entry by f-IFA

The phosphor-protein pp65 is the most abundant protein in the tegument layer of an incoming HCMV virion with its own nuclear location signal. pp65 enters the cell nucleus together with virus genome. For this reason, pp65 is often

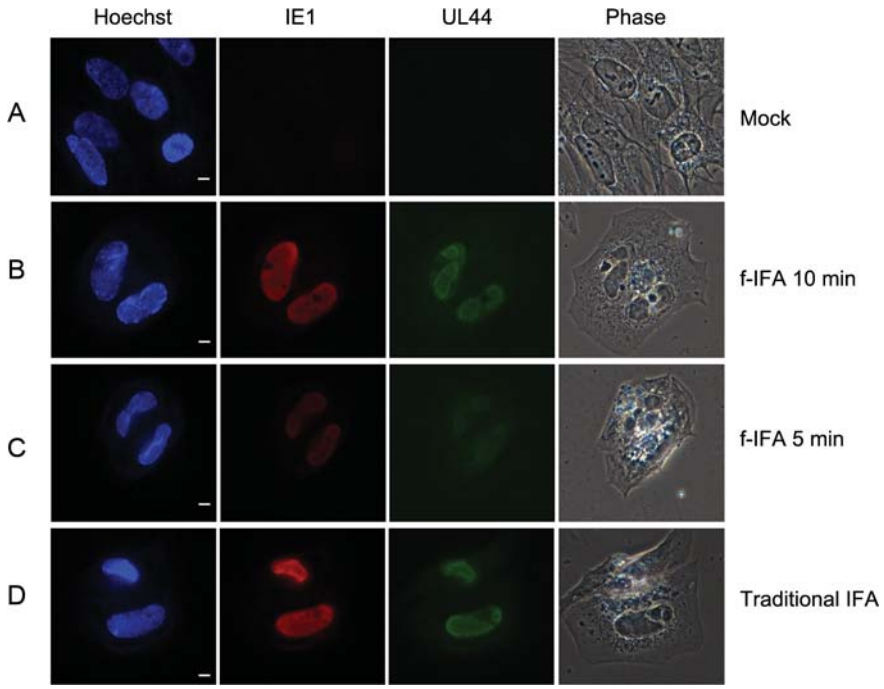


**Figure 2 HEL cells were mock-, virus-infected with Towne strain at an MOI of 5** Coverslips were collected at 48 h pi. By different staining ways samples were stained with anti-IE1, anti-UL44 antibodies, and their according secondary antibodies (TRITC-conjugated goat-anti-mouse IgG2a and Alexa 488-conjugated goat-anti-mouse IgG1). Nuclei were counterstained with Hoechst dye. (A) Mock-infected HEL stained by f-IFA. (B) Incubate with primary Ab and secondary Ab for 10 min, respectively, which is our standard f-IFA. (C) Shorter time incubation with primary Ab and secondary Ab for 5 min. (D) Follow the traditional IFA described in [4] and [5]. Briefly in a 12-well plate, blocking with 1 ml BS for 10 min followed by rinse twice with PBS, incubating with 1 ml primary Ab solution for 1 h followed by wash with PBS (5 min three times with shaking), then incubating with 1 ml secondary Ab solution for 1 h followed by wash with PBS (5 min three times with shaking). Scale bar = 5 μm.

used as an indicator of virus entry at the immediate-early stage [11–14]. To investigate the natural entry process, HEL cells were not synchronized to G0 by serum starving and infected with AD169 strain at an MOI of 5. **Figure 3** shows that in the mock-infected HEL cells, there was no pp65 staining signal. At 8 h pi, the pp65 signal presented as brighter punctuated spots in the cytoplasm, while it was weaker and evenly diffused in the nucleus; at 12 h pi, pp65 signals remained spotty in the cytoplasm, and the nucleus exhibited distinct staining signal.

### Tracking virus replication process by f-IFA

UL44 is the processivity factor of HCMV polymerase (UL54) and is expressed at the E phase pi. It localizes to the viral replication centers within the infected cell nuclei, and is a very good marker for visualizing the viral replication center. To reach synchronous infection, HEL cells were serum starved, and infected with HCMV (AD169 strain) at an MOI of 5, and stained for UL44 (**Fig. 4**). UL44 foci appeared as multiple small foci (by 24 h pi), then developed and fused to form bigger and bi-polar foci (by 48 h pi), finally developing into a single large focus within the nucleus (by 72 h pi), and over 90% of the foci were single large ones (by 96 h pi). As the infection proceeded, there were more granular particles observed in the cytoplasm in the phase images, especially in and around the viral assembly complex (**Fig. 4**, phase image at the bottom panel), which is consistent with viral replication center development. UL44 foci formation and development is an indicator of viral replication center formation and development, and it is also an indicator for tracking the viral infection progress. Increasing granular particles in the cytoplasm indicates virus assembly and trafficking from the nucleus to cytoplasm. All these results are consistent with observations on the progress of virus infection described previously [12,15–17].

### f-IFA is sensitive for the detection of HCMV infection

T98G cells are semi-permissive for HCMV infection, and infection in these cells is persistent/latent. Viral gene expression is very low, and antigen-positive T98G cells continue to divide instead of being arrested at G1/S or G2/M [8]. The total cell numbers and antigen-positive cell numbers were obtained from five fields on each coverslip (middle, left up/down, right up/down) and counted for 300–500 cells. To avoid bias during cell counting, we counted the cell nuclei (Hoechst counterstained) first, then counted the antigen-positive cells. The percentage was calculated by using the following formula:

$$\frac{\text{Number of Ag} - \text{positive cells}}{\text{Number of nuclei}} \times 100$$

Multiple-micronuclei, a hallmark of cell apoptosis, appeared in 0.5% of the HCMV-infected and IE1-positive T98G cells at passage 3 (P3, day 12 pi). A representative image is shown in **Fig. 5(A)**. Among the infected T98G cells, 2% had distinct advanced UL44 foci at P3 [**Fig. 5(B)**]. The existence of UL44 foci/replication centers indicates the potential for infectious virus to be manufactured and released. pp65 is synthesized *de novo* during virus replication and incorporated into infectious virions. The mature virions traffic from the nucleus through the cytoplasm via a viral assembly complex, finally being released at the plasma membrane [11–14]. Thus, tracking the trafficking of pp65-positive virions can confirm virus

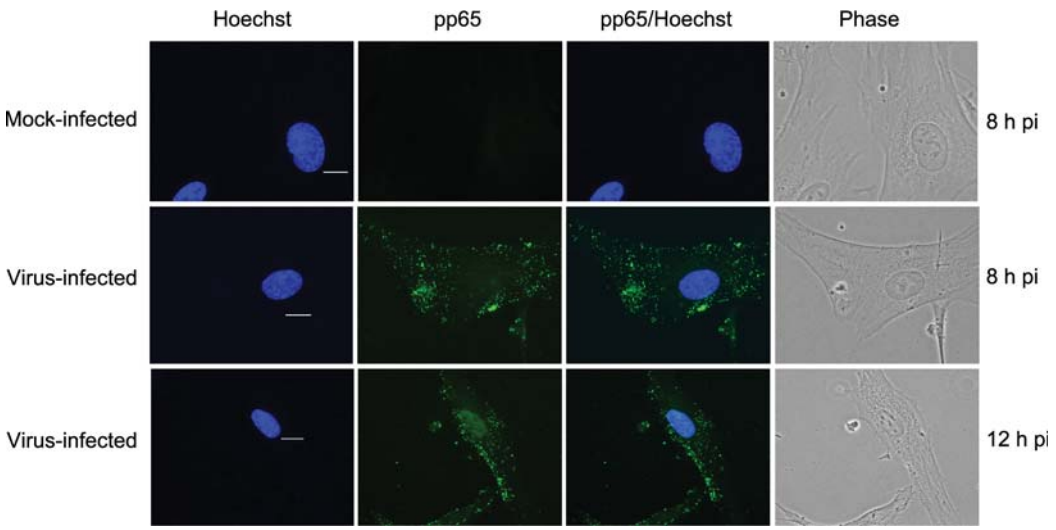


**Figure 3 Tracking of HCMV particle entry process by staining pp65** HEL cells are infected with HCMV (AD169 strain) at an MOI of 5, and coverslips are harvested at the indicated early time points. Samples were stained with anti-pp65 Ab. Mock-infected sample is shown in the top panel, virus-infected sample at 8 h pi in the middle panel, and 12 h pi in the bottom panel. Nuclei are counterstained with Hoechst dye for all images. Scale bar = 10 μm.

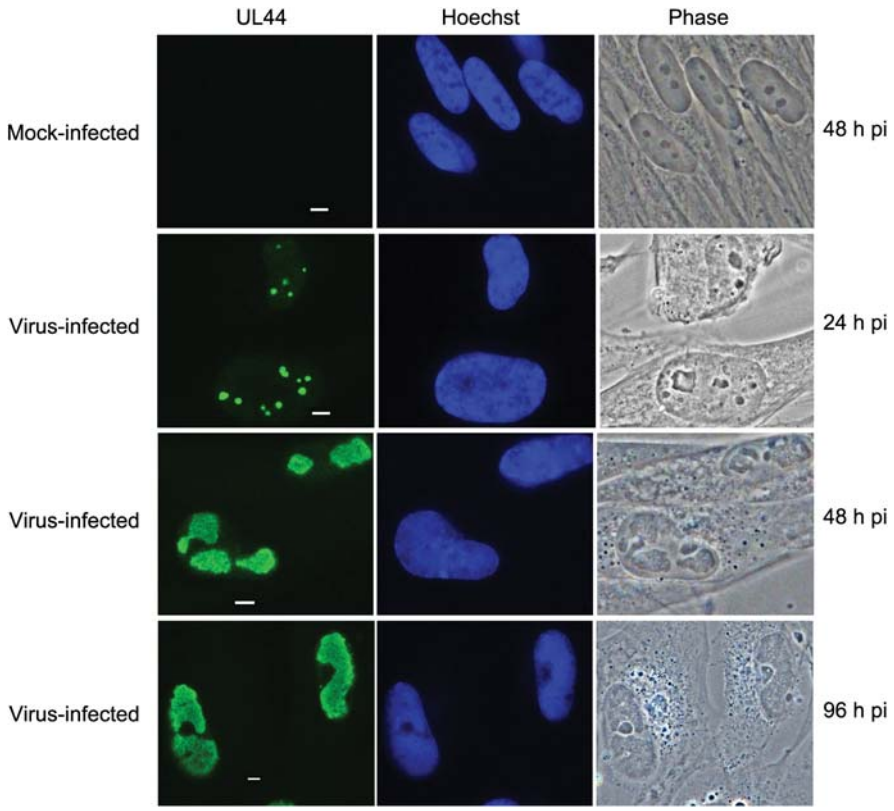


**Figure 4 Following the formation and development of HCMV replication centers by staining UL44** HEL cells were infected with HCMV (AD169 strain) at an MOI of 5. UL44 foci at different stages and different time points are shown. The foci develop from tiny points to bipolar foci then to a single large focus in a nucleus. Scale bar = 5 μm.

release. About 0.5% of the cells showed typical virus shedding as visualized pp65 staining via f-IFA [**Fig. 5(C)**]. All the T98G cells were infected by HCMV by using BrdU labeled virus as described previously [8]. Taken together, these results indicate that infection in T98G cells is different from that in fully permissive cells (e.g. HEL), and only a very low proportion of the infected cells had virus replication, which has not been observed in previous studies due to limitations in detection efficiency [18].

### Cytoskeleton collapse in HCMV-infected NPCs captured by f-IFA

NPCs are the most susceptible cells in the brain *in vivo* and fully permissive for CMV infection *in vitro* [6,10,19–21]. CMV infection causes neural cell loss, which is the direct reason for brain developmental disorders (e.g. microencephaly) [21,22]. However, it is very difficult to assess the neural cell loss induced by HCMV infection in autopsy brain tissue for pathological diagnosis. Glial filament acid protein (GFAP), a cytoskeleton protein, which is also a marker of NPCs, is down-regulated at both the mRNA and protein levels [10,23]. Here we used f-IFA to show the changes of GFAP pi (**Fig. 6**). At 4 h pi when it is at the very early stage of IE phase, GFAP was presented as blurry spots in the IE1-positive cells, and the filament structure was not as clear as in the IE1-negative cells [**Fig. 6(A)**]. As the infection progressed, the degree of break down of the GFAP filament became worse. GFAP appeared as bigger aggregated spots and the filament structure was totally destroyed until 72 h pi [**Fig. 6(B)**]. As GFAP is a marker and cytoskeleton protein of NPCs and the GFAP change is the CPE induced by HCMV infection, and IE1 is the marker for HCMV replication initiation, GFAP collapse in IE1-positive cells can therefore be used as a criterion for neural damage caused by HCMV infection. The HCMV IE1-negative cells with distinct GFAP filament structure were observed at the moment when a cell was in the process of division and the two daughter cells had not yet completely separated [**Fig. 6(A)**]. These features may benefit the diagnosis of HCMV infection in brain tissue. In addition, the cell was dividing asymmetrically with a larger and smaller nucleus, which indicates that one daughter cell will maintain progenitor/stem cell status and the other one will go into a differentiation program, and the differentiation may be induced by HCMV infection.

## Discussion

High-quality images for HCMV infection by f-IFA have been obtained from different HCMV-infected cells

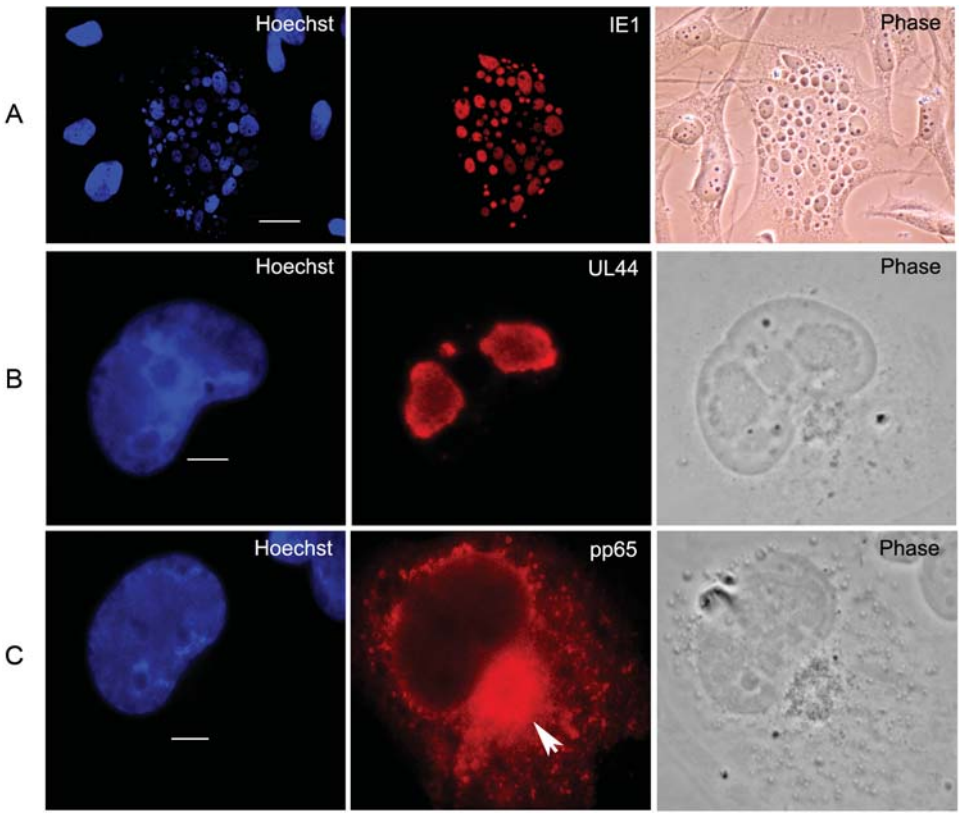


**Figure 5 IE1, UL44, and pp65 staining in HCMV (Towne strain)-infected T98G cells** (A) IE1-positive multi-micronuclei in HCMV-infected T98G cells, scale bar = 20 μm. (B) Distinct UL44 foci. (C) Virus shedding is visualized by pp65 staining. pp65-positive particles assembled at the virus assembly complex, which is visible as a large aggregate in the cytoplasm adjacent to the nucleus (indicated by a solid white arrow). Scale bar of (B) and (C) is 5 μm.

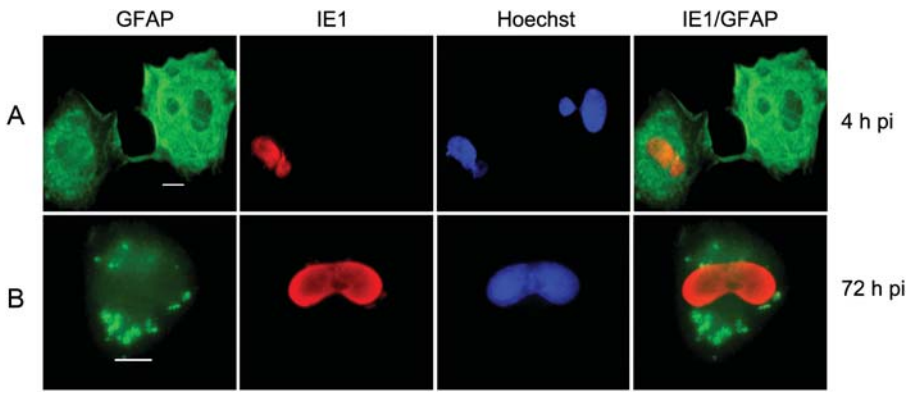


**Figure 6 HCMV collapsed GFAP structure in NPCs** NPCs were infected with HCMV (Towne strain), GFAP structure and HCMV IE1 expression were determined. (A) At 4 h pi, in the IE1-positive cell GFAP is spotty and the filament structure is unclear compared with the IE1-negative cells. (B) At 72 h pi, GFAP filament structure totally collapses; the total signal dramatically decreases; and most of the remaining signal is aggregated. Scale bar = 5 μm.

(**Figs. 2–6**), including fully permissive (HEL, NPCs) and semi-permissive (T98G) cells. Based on the results presented here and published previously [6–8,10,12], f-IFA is at least comparable to those obtained by IFAs [2–5,16,17,24].

The principal advantage of f-IFA is the speed of analysis with no accompanying trade-off in accuracy. f-IFA saves hours [6–8,10,12] compared with other IFAs [2–5,16,17,24]. The time-saving is primarily achieved by reducing the blocking time (15 min in f-IFA compared with hours in other IFAs) [5,25,26] and the primary and secondary Ab incubation steps (10 min for each incubation at RT instead of 0.5–3 h at 4°C in other IFAs) [4,5,25,26]. Additionally, time-saving is fulfilled by the efficient washing steps which are much faster and efficient than any other protocol [2–5,16,17,24].

A second benefit is that f-IFA requires much less Abs and is thus more cost-effective, as the incubation steps only

require 25 μl diluted Abs solution for each coverslip by placing the coverslips face down onto the solution. The dilution ratios of primary Abs are 1 : 1000 and the secondary Abs can be 1 : 5000, which is highly cost-effective for clinic application. All these time-saving and cost-effective conditions will benefit clinical application and high-quality images can be constantly obtained by f-IFA (**Figs. 2–6**).

Convenience is another benefit of f-IFA. The whole process is carried out at RT, obviating the need for a shaker, moisture chamber, 37°C incubator, or 4°C cold room. Our previous work has shown that high-quality fluorescent image was obtained by f-IFA [6–8,10,12], and these are comparable with other published results [2–5,16,17,24]. Because of the time-saving, cost-effective, and convenient advantages, this protocol could replace the other IFA protocols.

Virus entry and initiation of viral replication are the key steps for HCMV infection. The HCMV life cycle includes the following steps: virions enter into cells, tegument proteins (e.g. pp65), and viral genome travel into the nucleus; they set up viral replication centers and replicate in nuclei; finally, offspring virions are assembled in the viral assembly complex and then released at the cytoplasm membrane by budding. The initial event upon infection is virus entry and transportation into the nucleus. pp65 is the structural component of the virion that traffics and enters into the nucleus during virus entry. Thus, the virus entry process can be tracked with pp65 staining by f-IFA (**Fig. 3**). Furthermore, the virus sets up viral replication centers in the nucleus and these centers can be followed up and visualized with UL44 staining by f-IFA [**Figs. 4** and **5(B)**]. Formation of viral replication center in the nucleus indicates the potential for production of infectious virus offspring. Virus maturation and egress can also be tracked with pp65 staining by f-IFA [**Fig. 5(C)**]. Thus the infection process and details of virus entry and replication can be clearly and specifically determined by f-IFA.

Early and rapid diagnosis is a key component for effective infectious disease therapy. IFA is a commonly used scientific and diagnostic technology with a confirmed sensitivity and specificity. For HCMV infection, once the double-linear viral genome enters the nucleus, immediate-early gene products, the most commonly used viral specific marker for virus isolation and identification, are presented in the nucleus. IE1 is the first and most abundant among the IE gene products and clearly appears in NPCs nuclei at 4 h pi [**Fig. 6(A)**]. Dr Britt's group and others have used saliva and urine samples from newborn babies to diagnose HCMV congenital infection [27]. The samples were inoculated onto fibroblasts monolayer and cultured for 16 to 24 h, followed by IE1 determination by IFA. This method is used as an early and rapid diagnosis technology as well as the gold standard for diagnosis of virus infection in the clinic [27]. Using f-IFA, the diagnosis can be made faster and earlier since the IE1 signal is distinctly shown at 4 h pi [**Fig. 6(A)**]. Except for the potential application of f-IFA for early and rapid diagnosis of viral infection, it is also a more sensitive and specific method. Low occurrence events, such as multiple-micronuclei [**Fig. 5(A)**] and virus shedding [**Fig. 5(C)**] in HCMV-infected T98G cells, as well as asymmetrical cell dividing [**Fig. 6(A)**] are specifically captured by f-IFA.

In summary, this f-IFA is a faster, cost-effective, convenient technology with higher sensitivity and specificity. We have tracked the details of HCMV infection process (entry and viral replication) by f-IFA, the low incidence events are also captured during the infection. All these results suggest that f-IFA is suitable for early, rapid, and accurate diagnosis of virus infection, especially for HCMV infection.

## Acknowledgments

We are grateful to thank Prof. Zhan Yin (Institute of Hydrobiology, Chinese Academy of Sciences) for kindly providing the fluorescence microscope.

## Funding

This work was supported by the National Basic Research Program '973' (2011CB504804), the 'bai ren ji hua' Foundation (29Y002161YC1) from the Chinese Academy of Sciences, the National Natural Science Foundation of China (81071350, 31170155, 31000090), and a Seed Grant from the University of Idaho (YDP-764) to M.L. This work was also supported by NIH grants (# RO1- AI51463 and #P20 RR015587COBRE program) to E.F.

## References

1 Didier ES, Orenstein JM, Aldras A, Bertucci D, Rogers LB and Janney FA. Comparison of three staining methods for detecting microsporidia in fluids. J Clin Microbiol 1995, 33: 3138–3145.

2 Taber LH, Brasier F, Couch RB, Greenberg SB, Jones D and Knight V. Diagnosis of herpes simplex virus infection by immunofluorescence. J Clin Microbiol 1976, 3: 309–312.

3 Lee AW, Hertel L, Louie RK, Burster T, Lacaille V, Pashine A and Abate DA, *et al*. Human cytomegalovirus alters localization of MHC class II and dendrite morphology in mature Langerhans cells. J Immunol 2006, 177: 3960–3971.

4 Rogers SL and Rogers GC. Culture of Drosophila S2 cells and their use for RNAi-mediated loss-of-function studies and immunofluorescence microscopy. Nat Protoc 2008, 3: 606–611.

5 Strang BL, Boulant S and Coen DM. Nucleolin associates with the human cytomegalovirus DNA polymerase accessory subunit UL44 and is necessary for efficient viral replication. J Virol 2010, 84: 1771–1784.

6 Luo MH, Schwartz PH and Fortunato EA. Neonatal neural progenitor cells and their neuronal and glial cell derivatives are fully permissive for human cytomegalovirus infection. J Virol 2008, 82: 9994–10007.

7 Luo MH, Rosenke K, Czornak K and Fortunato EA. Human cytomegalovirus disrupts both ataxia telangiectasia mutated protein (ATM)- and ATM-Rad3-related kinase-mediated DNA damage responses during lytic infection. J Virol 2007, 81: 1934–1950.

8 Luo MH and Fortunato EA. Long-term infection and shedding of human cytomegalovirus in T98G glioblastoma cells. J Virol 2007, 81: 10424–10436.

9 Chen LY, Dai G, Wu GJ, Wang JW, Luo MH and Chen SZ. Influence of human cytomegalovirus infection on the expression of HOX genes in human embryo lung cells. Hunan Yi Ke Da Xue Xue Bao 2000, 25: 440–442.

10 Luo MH, Hannemann H, Kulkarni AS, Schwartz PH, O'Dowd JM and Fortunato EA. Human cytomegalovirus infection causes premature and abnormal differentiation of human neural progenitor cells. J Virol 2010, 84: 3528–3541.

11 Britt WJ and Vugler L. Structural and immunological characterization of the intracellular forms of an abundant 68,000 Mr human cytomegalovirus protein. J Gen Virol 1987, 68 (Pt 7): 1897–1907.

12 Casavant NC, Luo MH, Rosenke K, Winegardner T, Zurawska A and Fortunato EA. Potential role for p53 in the permissive life cycle of human cytomegalovirus. J Virol 2006, 80: 8390–8401.

13 Fortunato EA and Spector DH. p53 and RPA are sequestered in viral replication centers in the nuclei of cells infected with human cytomegalovirus. J Virol 1998, 72: 2033–2039.

14 Rosenke K and Fortunato EA. Bromodeoxyuridine-labeled viral particles as a tool for visualization of the immediate-early events of human cytomegalovirus infection. J Virol 2004, 78: 7818–7822.

15 Iwayama S, Yamamoto T, Furuya T, Kobayashi R, Ikuta K and Hirai K. Intracellular localization and DNA-binding activity of a class of viral early phosphoproteins in human fibroblasts infected with human cytomegalovirus (Towne strain). J Gen Virol 1994, 75 (Pt 12): 3309–3318.

16 Mocarski ES, Pereira L and Michael N. Precise localization of genes on large animal virus genomes: use of lambda gt11 and monoclonal antibodies to map the gene for a cytomegalovirus protein family. Proc Natl Acad Sci USA 1985, 82: 1266–1270.

17 Penfold ME and Mocarski ES. Formation of cytomegalovirus DNA replication compartments defined by localization of viral proteins and DNA synthesis. Virology 1997, 239: 46–61.

18 Jault FM, Spector SA and Spector DH. The effects of cytomegalovirus on human immunodeficiency virus replication in brain-derived cells correlate with permissiveness of the cells for each virus. J Virol 1994, 68: 959–973.

19 Cheeran MC, Hu S, Ni HT, Sheng W, Palmquist JM, Peterson PK and Lokensgard JR. Neural precursor cell susceptibility to human cytomegalovirus diverges along glial or neuronal differentiation pathways. J Neurosci Res 2005, 82: 839–850.

20 Melnick M, Mocarski ES, Abichaker G, Huang J and Jaskoll T. Cytomegalovirus-induced embryopathology: mouse submandibular salivary gland epithelial-mesenchymal ontogeny as a model. BMC Dev Biol 2006, 6: 42.

21 Shinmura Y, Kosugi I, Kaneta M and Tsutsui Y. Migration of virus-infected neuronal cells in cerebral slice cultures of developing mouse brains after in vitro infection with murine cytomegalovirus. Acta Neuropathol 1999, 98: 590–596.

22 Odeberg J, Wolmer N, Falci S, Westgren M, Sundtrom E, Seiger A and Soderberg-Naucler C. Late human cytomegalovirus (HCMV) proteins inhibit differentiation of human neural precursor cells into astrocytes. J Neurosci Res 2007, 85: 583–593.

23 Shinmura Y, Aiba-Masago S, Kosugi I, Li RY, Baba S and Tsutsui Y. Differential expression of the immediate-early and early antigens in neuronal and glial cells of developing mouse brains infected with murine cytomegalovirus. Am J Pathol 1997, 151: 1331–1340.

24 Ranneberg-Nilsen T, Dale HA, Luna L, Slettebakk R, Sundheim O, Rollag H and Bjoras M. Characterization of human cytomegalovirus uracil DNA glycosylase (UL114) and its interaction with polymerase processivity factor (UL44). J Mol Biol 2008, 381: 276–288.

25 Bhattacharyya D, Hammond AT and Glick BS. High-quality immunofluorescence of cultured cells. Methods Mol Biol 2010, 619: 403–410.

26 Schneider Gasser EM, Straub CJ, Panzanelli P, Weinmann O, Sassoe-Pognetto M and Fritschy JM. Immunofluorescence in brain sections: simultaneous detection of presynaptic and postsynaptic proteins in identified neurons. Nat Protoc 2006, 1: 1887–1897.

27 Boppana SB, Ross SA, Shimamura M, Palmer AL, Ahmed A, Michaels MG and Sanchez PJ, *et al*. Saliva polymerase-chain-reaction assay for cytomegalovirus screening in newborns. N Engl J Med 2011, 364: 2111–2118.